

Nanoassemblies formed from hydrophilic block copolymers and multivalent ions†

Nicolas Sanson,^a Frédéric Bouyer,^a Corine Gérardin^{*a} and Martin In^b

^a UMR5618 CNRS-Ecole Nationale Supérieure de Chimie de Montpellier, 34296 Montpellier, France. E-mail: gerardin@cit.enscm.fr; Fax: 33 (0)46716 3470; Tel: 33 (0)46716 3465

^b Groupe de Dynamique des Phases Condensées, Université Montpellier II, France

Received 11th November 2003, Accepted 19th February 2004
First published as an Advance Article on the web 3rd March 2004

We recently reported on the controlled formation of highly stable metal hydroxide nanoparticles. Growth control and stabilization of particles were achieved by performing hydrolysis and polycondensation reactions of polymer-complexed metal cations, the polymers being double hydrophilic block copolymers (DHBCs). The present paper focuses on the characterization of the intermediate species in the formation process, namely the mixture of multivalent metal cations plus the oppositely charged polyelectrolyte–neutral block copolymers. Complexation of metal cations by the anionic block of the DHBCs leads to the spontaneous formation of colloidal objects. Small angle neutron scattering experiments show that the aggregates exhibit a well defined core–corona architecture: the core is compact and homogeneous while the diffuse corona is constituted of polymer segments in a good solvent. The core formation is due to the water insoluble metal cation–polyacrylate complex while the corona is constituted of the water soluble neutral polymer blocks. Cryo-TEM images allowed the revelation of well-dispersed inorganic-rich domains. The presence of the longer neutral blocks prevents macroscopic phase separation of the complex and leads to the formation of hybrid micellar aggregates.

Introduction

The recent development of nanoparticle-based materials has ushered in a need for reliable preparation routes for stable nanoparticles of controlled properties. The most important characteristics of nanoparticles are their size, shape, chemical composition, structure and stability. Colloidal particles of metal hydrous oxides have various applications depending on the nature of the metal ion; they are most commonly prepared by hydrolysis of metal cations in the presence of small complexing agents. We have recently shown that it was possible to prepare highly stable suspensions of metal hydroxide-based particles with tunable sizes by using well-chosen double hydrophilic block copolymers (DHBC).¹ DHBCs have recently known a considerable development; a review on their synthesis and applications was recently published by Cölfen.² DHBCs containing an anionic complexing block and a neutral block can be used to simultaneously ensure growth and stabilization control of metal hydroxide nanoparticles.¹ The controlled formation of metal hydroxide particles was illustrated by the cases of Cu²⁺, Al³⁺, La³⁺ metal ions.^{3,4} The formation of M(OH)_n phases is induced by hydroxylation of metal ions and polycondensation reactions in the presence of the polymers. Metal cationic precursors can be either Mⁿ⁺ metal ions (*n* = 2, 3...) or polycations⁵ such as the Keggin tridecamer Al₁₃⁷⁺ or Al₃₀¹⁸⁺ or nanoparticles obtained by controlled partial prehydrolysis of metal ions. The block copolymers contain an ionizable block, which is polyacrylic acid, and a neutral block which can be polyhydroxyethylacrylate or polyacrylamide.

A detailed investigation of the particle formation mechanisms is necessary in order to better control the particle properties. Our goal was then to characterize the intermediate species in the formation process. When anionic–neutral DHBC are

mixed with metal cations, the spontaneous formation of colloidal objects is observed. These aggregates are the precursors for polymer-stabilized inorganic nanoparticles; it is important to characterize them since the characteristics (size, shape) of the resulting metal hydroxide-based particles are a direct function of the characteristics of the precursor aggregates.^{3,4} In this paper, we want then to report on the characteristics of these colloidal aggregates formed between multivalent metal cations and oppositely charged block copolymers. The sizes, shapes and microstructures of the cation/copolymer aggregates were examined by using dynamic light scattering (DLS) and small angle neutron scattering (SANS) together with cryo transmission electron microscopy (cryo-TEM). The colloidal stability of the nanoassemblies was also investigated. In this paper, only the case of asymmetric block copolymers constituted of a functional anionic block smaller than the neutral block is treated.

Experimental

Solutions of Al(NO₃)₃·9H₂O (Aldrich) in water were used as Al³⁺ salt solutions. Pure solutions of Al₁₃⁷⁺ clusters were prepared by controlled prehydrolysis of Al³⁺ solution (0.1 M) with sodium hydroxide solutions (0.3 M) at 90 °C. A prehydrolysis ratio *h*₁ = [OH⁻]/[M] of 2.46 was used. It was checked by ²⁷Al NMR that the solution contained only Al₁₃ species. Ultrapure deionized water (MilliQ, Millipore, France) was used for all solution preparations.

The block copolymers used in this study are polyacrylic acid (PAA)-b-polyhydroxyethylacrylate (PHEA) or polyacrylic acid (PAA)-b-polyacrylamide (PAM), whose molecular weights (g mol⁻¹) are indicated close to each block name in the following. PAA-b-PAM and PAA-b-PHEA block copolymers were provided by Rhodia (Aubervilliers, France), their synthesis was described earlier.⁶ Before mixing the copolymer with solutions of metal ions, the pH of the copolymer solution is adjusted to 5.5, which means a dissociation degree of acrylic

† Presented at the 17th Conference of the European Colloid & Interface Science Society, Firenze, Italy, September 21–26, 2003.

acid functions of about 50%. Specifications of polymers used in the present work are indicated in Table 1.

The hybrid nanoaggregates described in this paper are prepared by adding copolymer solutions (5 wt.%) into metal ions containing solutions, under fast stirring at room temperature. Metal concentrations in the final suspensions vary between 5×10^{-3} and 10^{-1} M.

Dynamic light scattering experiments were run using a Malvern spectrogoniometer, Autosizer 4800, with a 50 mW laser source operating at 532 nm. Hydrodynamic sizes were measured at 90° .

SANS experiments were run at Laboratoire Leon Brillouin (Saclay, France), on the PACE beam line. A q (magnitude of the wave vector)-range from 0.004 to 0.45 \AA^{-1} was covered by collecting the data at two distances $d = 1$ m and 3 m, with respective incident neutron wavelengths of 5 Å and 10 Å. Suspensions for SANS measurements were prepared in D_2O to enhance the scattering length density differences between the particles and the solvent. Al_{13}^{7+} clusters were synthesized in D_2O ; then, the $\text{Al}_{12}(\text{AlO}_4)(\text{OD})_{24}(\text{D}_2\text{O})_{12}^{7+}$ species have scattering length densities similar to the scattering length density of D_2O . Samples were introduced into 2 mm thick quartz cells for analysis.

TEM images were recorded using a Philips CM200 'Cryo' microscope operated at 80 kV. Cryo-TEM samples were prepared by quench-freezing a thin film of the colloidal suspension into liquid ethane cooled to -171°C . The specimen was mounted onto a Gatan 626 cryo-holder and transferred into the microscope. The colloids were observed at low temperature (-180°C) embedded in a thin layer of vitreous ice.

Results and discussion

Before studying the aggregates formed from polymers and multivalent ions, the characteristics of polymers in water were examined. This study was necessary in order to investigate the polymer conformations in the absence of multivalent metal ions. It is well known that hydrogen bonds can form between acrylamide and acrylic acid functions leading to chain aggregation.

SANS measurements were, then, run on polymers in solution in the absence of metal ions and polymer solubility was investigated at pH 5.5. Fig. 1 shows SANS curves for a series of PAA-b-PHEA polymers, whose molecular weights of the two blocks are indicated in the figure. The scattered intensities are plotted as a function of the amplitude of the scattering vector, q . The polymer weight concentrations of the samples vary between 17% and 20%, but the scattered intensities reported on Fig. 1 were normalized at the same polymer

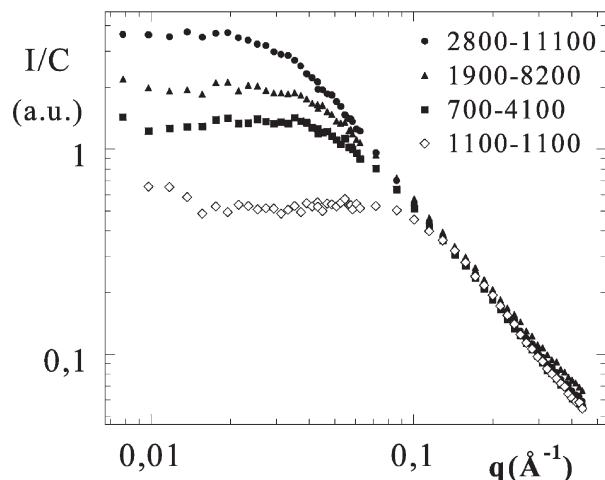


Fig. 1 SANS curves for a series of PAA-b-PHEA polymers of different molecular weights, normalized at the same polymer weight fraction.

weight concentration. The slopes at high q values are close to 1.7, which is characteristic of polymers in a good solvent, with excluded volume effects. In that high q domain, all scattering curves, normalized at the same polymer concentration, superimpose, suggesting that all polymers have the same solubility in water. The radii of gyration were determined by Guinier approximation $I(q) = I(0)\exp(-q^2 R_G^2/3)$ for PAA-b-PHEA polymers presented in Fig. 1. It was observed that they do not depend on the polymer weight concentration. A power law relation was obtained between the radii of gyration and the total polymer molecular weights: $R_G \propto M_w^{0.62}$, as shown in Fig. 2. The value of the power exponent corresponds to what is expected for water-soluble macromolecules with excluded volume effects. The present results exclude any assembly phenomenon between polymers due to hydrogen bonding between block units. Characterization of the polymers confirm that the DHBCs behave as soluble polymers and do not self-assemble.

The suspensions obtained by mixing of block copolymers and multivalent cations are characterized by the metal complexation degree R , which is the number of acrylate functions added per metal atom ($R = [\text{AA}]/[\text{M}]$). Complexation of metal cations by acrylate groups leads to the spontaneous formation of objects larger than the initial polymer coil sizes. Hydrodynamic diameters, D_h , of the aggregates were measured by dynamic light scattering. As indicated in Table 2 with a series of PAA-b-PHEA copolymers, the hydrodynamic diameters of aggregates increase with the total molecular

Table 1 Specifications of three PAA-b-PHEA block copolymers used in the present study: molecular weights and number of monomers of the two blocks

Ionizable block	Neutral block
PAA	PHEA
$\begin{array}{c} \text{PAA} \\ \text{-(CH}_2\text{-CH)}_n\text{-} \\ \quad \\ \quad \text{C=O} \\ \quad \\ \quad \text{OH} \end{array}$	$\begin{array}{c} \text{PHEA} \\ \text{-(CH}_2\text{-CH)}_n\text{-} \\ \quad \\ \quad \text{C=O} \\ \quad \\ \quad \text{O-CH}_2\text{-CH}_2\text{-OH} \end{array}$
$M_w(\text{PAA})/n(\text{AA})$ (g mol^{-1})	$M_w(\text{PHEA})/n(\text{HEA})$ (g mol^{-1})
900/12	9200/88
1900/26	8200/79
2800/39	11100/107

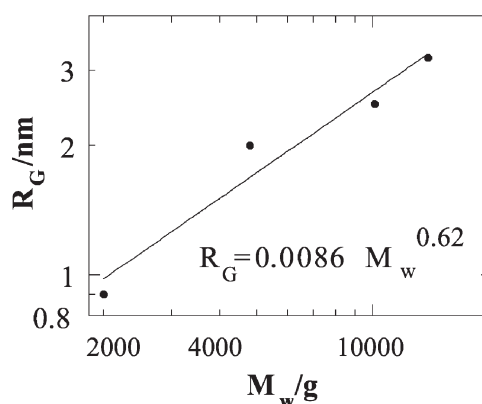


Fig. 2 Variation of the radii of gyration of the PAA-b-PHEA block copolymers with the total molecular weights (same polymers as in Fig. 1).

Table 2 Radii of gyration (determined by SANS), hydrodynamic diameters (determined by dynamic light scattering) and particle diameters by TEM of micellar aggregates formed from Al_{13}^{7+} and different asymmetric block copolymers, at a complexation degree $R = 1$, $[\text{AA}] = [\text{Al}] = 10^{-2}$ M

Aggregate Al_{13}^{7+} /PAA-b-PHEA $M_w/\text{g mol}^{-1}$	900–9200	1900–8200	2800–11 100
R_G/nm	9.0	10.7	12.6
D_h/nm	22	41	47
Particle diameter by TEM/ nm	—	7	9

weight. Typically, the size of the aggregate formed from Al_{13}^{7+} and PAA 1900-b-PHEA 8200, $R = 1$, (see Table 2) equals $D_h = 41$ nm, which is almost 4 times bigger than the hydrodynamic diameter of the corresponding copolymer in solution (11 nm). The aggregate size does not considerably change with the acrylate to metal molar ratio, R , in the range of R values varying from 0.1 to 5. This result suggests cooperative aggregation of the polymers.

SANS experiments were run to characterize the nanostructure of the induced assemblies. Fig. 3 shows the scattering curve of an aggregate from Al_{13}^{7+} and PAA 1900-b-PHEA 8200 ($R = 1$), together with the scattering curve of the same copolymer in water. The scattered intensities of the samples are plotted at the same copolymer concentration, in the absence and in the presence of polycations. As Al_{13}^{7+} clusters were synthesized in D_2O solvent, the $\text{Al}_{12}(\text{AlO}_4)(\text{OD})_{24-}(\text{D}_2\text{O})_{12}^{7+}$ species have a scattering length density ($6.6 \times 10^{-10} \text{ cm}^{-2}$) that practically matches that of D_2O ($6.38 \times 10^{-10} \text{ cm}^{-2}$). Then, the scattered intensity of the cation/polymer mixture essentially arises from the polymer blocks. The comparison of the two curves in Fig. 3 clearly evidences the formation of polymer aggregates upon addition of multivalent ions. At low q values, the observation of a scattered intensity higher for the suspension with polycations than that of the polymer solution supports the formation of polymer nanoassemblies. The radii of gyration R_G of the copolymer on one hand, and of the aggregate, on the other hand, were determined. In the case described in Fig. 3, R_G equals 11 nm for assemblies of PAA 1900-b-PHEA 8200 with Al_{13}^{7+} ($R = 1$), this can be compared to the radius of gyration of the copolymer in solution, which equals 2.5 nm, as determined by the Guinier approximation. Table 2 gives the radii of gyration of aggregates formed from Al_{13}^{7+} and different PAA-b-PHEA polymers. When increasing the copolymer length, the radius of gyration of the resulting aggregates increases. From the ratio between the intensity at the Guinier plateau (I_G) scattered

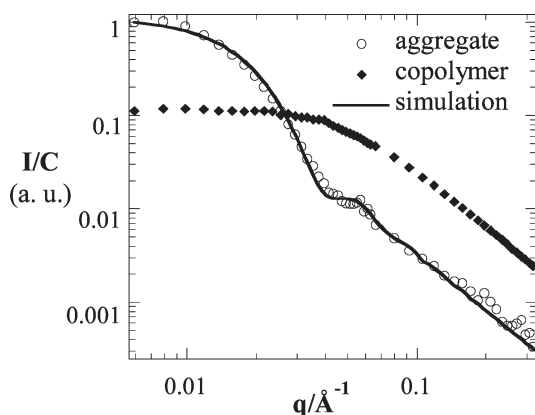


Fig. 3 SANS curves of the micellar aggregate ($[\text{AA}] = [\text{Al}] = 10^{-2}$ M) formed from Al_{13}^{7+} and PAA 1900-b-PHEA 8200, and of the copolymer in water, at the same polymer weight concentration.

by the aggregate and the intensity I_G scattered by the polymer (the two curves being normalized at the same polymer concentration), it was possible to estimate the aggregation number N_{agg} of the assemblies (number of copolymers forming one micellar aggregate). In the case described in Fig. 3 (PAA 1900-b-PHEA 8200 and Al_{13}^{7+} , $R = 1$), N_{agg} equals 9.

The high q -range of the scattering curve (Fig. 3) characterizes the interface between the micelle and the solvent. In that q -domain, a power law behaviour of the intensity, $I(q) \propto q^{-1.7}$, shows that the interface between the micelle and the solvent is constituted of a diffuse corona of polymeric chains in a good solvent. The power exponent of 1.7 is in good agreement with an excluded volume model considering self-avoidance and mutual avoidance of the corona chains. In this high q value domain, the scattered intensity from the aggregate is smaller than the intensity scattered by the polymer solution without multivalent ions. Observation of a decrease in surface area of the suspension is consistent with the formation of nanoaggregates. The similarity in the slopes of $I(q)$ at high q values of the curves of the copolymer and of the aggregate is consistent with the small value of the aggregation number: the chains in the corona are not stretched, they are not more elongated than they are when the copolymer is in solution.

An interesting point is that the scattering curve of the aggregate presents a sharp decrease of the intensity ($I(q) \propto q^{-3.9}$) in the intermediate q -range ($0.025 \text{ \AA}^{-1} < q < 0.045 \text{ \AA}^{-1}$). This suggests that the core, which is formed from cations and the collapsed polyelectrolyte blocks, is well-defined and presents a rather sharp interface with the surrounding corona. The aggregate scattering curve was simulated (Fig. 3) using Pedersen's model^{7,8} that was developed for form factors of core-corona micelles of block copolymers. This model considers that the scattering object is constituted of a sphere of homogeneous density, surrounded by gaussian chains attached to it. The gaussian chains are generated as random walks in three dimensions starting at the surface of the sphere. The simulation of the experimental data is presented on Fig. 3, it shows that the model allows the structure of the present hybrid aggregate to be correctly described. Nevertheless, because of the use of gaussian statistics for the corona chains in the model, a slight difference in slopes is observed at high q values. The model gives a q^{-2} dependence of the intensity, whereas the experimental curves present smaller exponents ($I(q) \sim q^{-1.7}$). This leads to a slight discrepancy, which is observed at higher q values, and that is due to the fact that excluded volume interactions between the chains were neglected.

Also, from the simulated curve, we can conclude that the aggregate core must be isotropic but we cannot affirm that it is spherical. SANS data showed that the nanoaggregates are constituted of homogeneous small cores surrounded by a corona of chains in a good solvent.

The small values of R_G/R_h (close to 0.5 for aggregates of Al_{13}^{7+} with PAA 1900-b-PHEA 8200 and PAA 2800-b-PHEA 11 100) support the core-corona architecture of the aggregates.

Fig. 4 shows a cryo-TEM image of micelles formed from Al_{13}^{7+} and PAA 2800-b-PHEA 11 100. The image evidences a controlled microphase separation with well separated isotropic objects. The particles observed by TEM present a small size distribution around a mean diameter of 9 nm; in the case of the system Al_{13}^{7+} and PAA 1900-b-PHEA 8200 (TEM image not shown here), the mean size equals about 7 nm (as reported in Table 2). TEM images reveal that inorganic ions are segregated in small domains in the central part of the aggregates.

The different characterization results lead to the following description: the nanoassemblies are constituted of a central core formed from the insoluble metal polyacrylate complex and a corona of water-soluble neutral polymeric segments; the interface between the inorganic-rich core and the corona is rather sharp and well-defined. A schematic representation of the hybrid micellar aggregates is then given in Fig. 5.

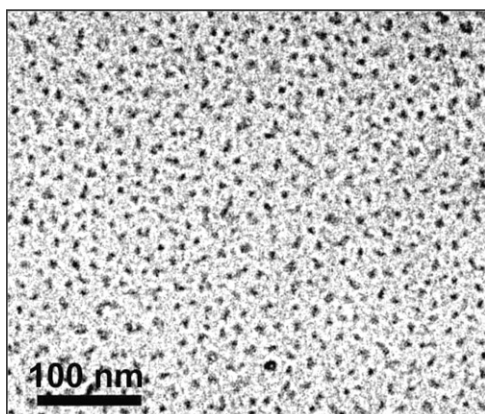


Fig. 4 Cryo-TEM image of aggregates formed from Al_{13}^{7+} and PAA 2800-b-PHEA 11 100 ($[\text{AA}] = [\text{Al}] = 10^{-2}$ M).

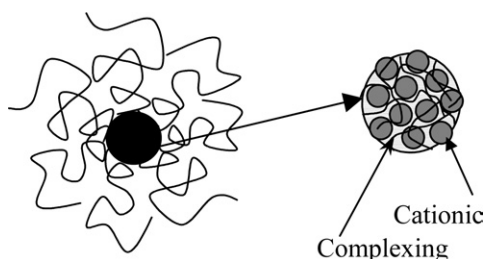


Fig. 5 Schematic representation of the hybrid micellar aggregates from metal cations and anionic DHBCs.

The stability of the colloids was investigated. It was observed that the colloidal complexes are very stable with time (for months). The neutral polymer segments constitute an effective barrier against particle aggregation. Suspension stability does not suffer from a change in concentration, neither an increase in electrolyte concentration. The concentration of monovalent ions (KCl, NaNO_3) in the suspensions could be increased up to 2.8 M while the colloids remain stable and keep the same size. The formation of coordination bonds between metal ions and acrylate groups within the core makes the aggregate stable towards salt addition.

Several asymmetric anionic–neutral block copolymers and different multivalent ions (Ca^{2+} , Cu^{2+} , Zn^{2+} , Ni^{2+} , Al^{3+} , La^{3+} ... and polycations) were used to prepare nanoassemblies. The neutral block could be polyacrylamide or polyhydroxyethylacrylate. When the ratio between the molecular weight of the neutral block relative to that of the polyacrylate block is higher than 3, the aggregates present similar structural characteristics. The microstructure described here is similar to that of core–corona micelles formed from amphiphilic block copolymers in a selective solvent.^{9,10} In the present case, the formation of core–corona structures is explained by the formation of an insoluble complex, whose macroscopic precipitation is inhibited by the presence of long neutral blocks. It is well known that in the presence of multivalent ions, oppositely charged homopolymers precipitate into compact structures.¹¹ In the case of DHBCs, macroscopic phase separation is prevented; neutral blocks sterically stabilize the water-incompatible phase giving rise to the formation of micellar-like structures. The formation of supramolecular structures of DHBC was reported in literature in the case of formation of polyion complex (PIC) micelles from charged diblock copolymers with oppositely-charged polymers or surfactants.^{12,13,14,15} The formation of aggregates between DHBC and metal ions was also reported by several authors.^{16,17} The hybrid

analogues of the PIC micelles, which are described here, present a major stability difference with PIC aggregates. In the case of polymer PIC micelles, the complex formation is essentially triggered by electrostatic interaction and entropy gain for the released counter-ions of the polymers. In the case of metal cations, the formation of coordination bonds is an additional factor of stability; inorganic/polymeric micelles are then very stable towards salt addition, in contrast to polymer–polymer or polymer–surfactant micelles.

In conclusion, the present results lead us to consider the complex system [hydrophilic diblock copolymer + multivalent ion] as an amphiphilic entity giving rise to stable hybrid micellar nanoaggregates. As it was shown earlier, the hybrid micelles represent new supramolecular precursors for inorganic polycondensation reactions; they can lead to the formation of highly stable suspensions of nanoparticles. Metal hydroxide particles were prepared using metal cations and hydrophilic complexing copolymers but the present hybrid micelles are also excellent candidates for the preparation of colloids of inorganic salts such as calcium carbonates, calcium phosphates or barium sulfate... It should also be mentioned that the present hybrid micelles can serve as model systems for reactions in confined environments.

Acknowledgements

One of the authors acknowledge financial support provided by Rhodia. The authors thank M. Destarac (Rhodia Aubervilliers, France) for providing the copolymers, L. Auvray for his help in neutron scattering measurements, at the Laboratoire Léon Brillouin, Saclay, France and J. L. Putaux (Grenoble, France) for cryo-TEM experiments.

References

- 1 C. Gérardin, N. Sanson, F. Bouyer, F. Fajula, J.-L. Putaux, M. Joanicot and T. Chopin, *Angew. Chem. Int. Ed. Engl.*, 2003, **42**, 3681–3685.
- 2 H. Cölfen, *Macromol. Rapid Commun.*, 2001, **22**, 219–252.
- 3 F. Bouyer, C. Gérardin, F. Fajula, J.-L. Putaux and T. Chopin, *Colloid. Surf. A*, 2003, **217**(1–7), 179–184.
- 4 C. Gérardin, V. Buisette, F. Gaudemet, O. Anthony, N. Sanson, F. DiRenzo and F. Fajula, *Mater. Res. Soc. Symp. Proc.*, 2002, **726**, Q7.5.
- 5 L. Allouche, C. Gérardin, T. Loiseau, G. Férey and F. Taulelle, *Angew. Chem. Int. Ed. Engl.*, 2000, **39**(3), 511–514.
- 6 D. Taton, A.-Z. Wilczewska and M. Destarac, *Macromol. Rapid Commun.*, 2001, **22**, 1497–1503.
- 7 J. S. Pedersen and M. C. Gerstenberg, *Macromolecules*, 1996, **29**, 1363.
- 8 J. S. Pedersen and C. Svaneborg, *Curr. Opin. Colloid Interface Sci.*, 2002, **7**, 158.
- 9 S. Förster, N. Hermsdorf, C. Böttcher and P. Lindner, *Macromolecules*, 2002, **35**, 4096–4105.
- 10 I. W. Hamley, J. S. Pedersen, C. Booth and V. M. Nace, *Langmuir*, 2001, **17**, 6386.
- 11 C.-I. Huang and M. Olvera de la Cruz, *Macromolecules*, 2002, **35**(3), 976–986.
- 12 A. V. Kabanov, T. K. Bronich, V. A. Kabanov, K. Yu and A. Eisenberg, *Macromolecules*, 1996, **29**, 6797.
- 13 A. Harada and K. Kataoka, *Science*, 1999, **283**, 65.
- 14 P. Hervé, M. Destarac, J.-F. Berret, J. Lal, J. Oberdisse and I. Grillo, *Europhys. Lett.*, 2002, **58**(6), 912.
- 15 J.-F. Berret, P. Hervé, O. Aguerre-Chariol and J. Oberdisse, *J. Phys. Chem. B*, 2003, **107**(32), 8111–8118.
- 16 L. M. Bronstein, S. N. Sidorov, P. Valetsky, J. Hartmann, H. Colfen and M. Antonietti, *Langmuir*, 1999, **15**, 6256.
- 17 Y. Li, Y.-K. Gong, K. Nakashima and Y. Murata, *Langmuir*, 2002, **18**, 6727.